Natural Science Report, Ochanomizu University, Vol. 12, No. 1, 1961
お茶の水女子大学 自然科学報告 第12巻 第1号

On the Analyses of the Data of the Tokai Experiments

Jiro Sakagami (坂上治郎)

Department of Physics, Faculty of Science,
Ochanomizu University, Tokyo

Abstract

A series of field experiments had been carried out at Tokai since 1958 by the members of the Investigation Committee for Atomic Energy and Meteorology. The data were analysed in detail. The complicated results of the horizontal concentration profiles were fairly explained by the assumption that they were caused by the changes of mean wind directions over the whole field of the experiments. The Pasquill's method and the Sutton's formula were discussed. However, the author's formula seemed to be more adequate compared with them.

Introduction

In order to obtain experimental data concerning the atmospheric diffusion, especially to obtain fundamental informations on the diffusion in the neighbourhood of Tokai where some atomic furnaces for research have been constructed and the first industrial atomic furnace in our country is going to be constructed, the Investigation Committee for Atomic Energy and Meteorology had carried out some field experiments since August 1958. Some reports have already been published.[1) 2)] We have made detailed analyses of the data obtained in the Prairie Grass Project,[3)] so we intended to analyse the data obtained in the Tokai experiments on the same line.

Among the experimental data, those obtained in February and in June 1959 are the most adequate ones to be analysed in detail. However, as the experiments in February were the preliminary ones for those in June, and they were carried on the scale within 300 m leeward, we have analysed chiefly the data obtained in June.[(1)]

Field instrumentation

In the experiments in June, ice crystals of PbI_2 were emitted from a stack whose height was 65 m above the ground and which

(1) The experiments in February were directed by Prof. G. Yamamoto, Tohoku Univ. and those in June were directed by Dr. S. Kawabata, Meterological Agency, and the members of some organizations joined togather for the experiments. The author also has cooperated for the analysis of the data.

was built attached to the tower for meteorological observations in the Research Institute of Atomic Energy. The air contaminated with the crystals was gathered in pilot balloons (200 g) by bellows, then the concentrations in the balloons were measured by the measuring apparatus for ice crystals. The sampling time was 10 minutes and air of about 200 l was gathered in the balloon,[2][3] and the sampling height was 1.5 m above the ground.

On 500m, 900 m and 3 km arc 5, 10 and 20 observation posts were selected respectively in a 90° sector whose central axis was directed to the mean wind direction (Fig. 1).

Wind speeds and directions were observed by aerovanes set to the observation tower at 10, 40 and 65 m above the ground, and quick running records were obtained in some periods at 65 m.

At two places, 2 km apart from the source respectively, wind speeds and directions in every 100 m up to 1000 m above the ground were observed by pilot ballons.

Air temperatures at 0.5, 10, 20 and 40 m above the ground were observed by Assmann's thermometers before and after each experiment. At 2 km NNW from the source, temperature profiles were observed by a tied balloon during each experiment.

Furthermore, a bivane which was tentatively made in the Research Institute for Agricultural Sciences was set at the height of 40 m of the tower.

The summary of the conditions of the experiments is shown in Table 1.

Results of the experiments

Results of the measurements of the concentrations (χ) are shown in Figs. 2~5. It is obvious from these figures that the five posts on the 500 m arc were too distant each other for the concentration measurements.

In order to make clear the essential characteristics of the profiles, we plotted $\log \chi$ on each arc against angular distances of the measuring posts, and considering that the mean wind directions might change with the distance, we shiftted the curves along the abscissa and, putting aside the decrease of the concentration with the distance, we shiftted the curves along the ordinate, so we obtained Figs. 6~9.

(2) Only on June 4, the sampling time was 20 minutes.

(3) The releasing, sampling and concentration measurements of the ice crystals were directed by Prof. K. Isono, Tokyo Univ.

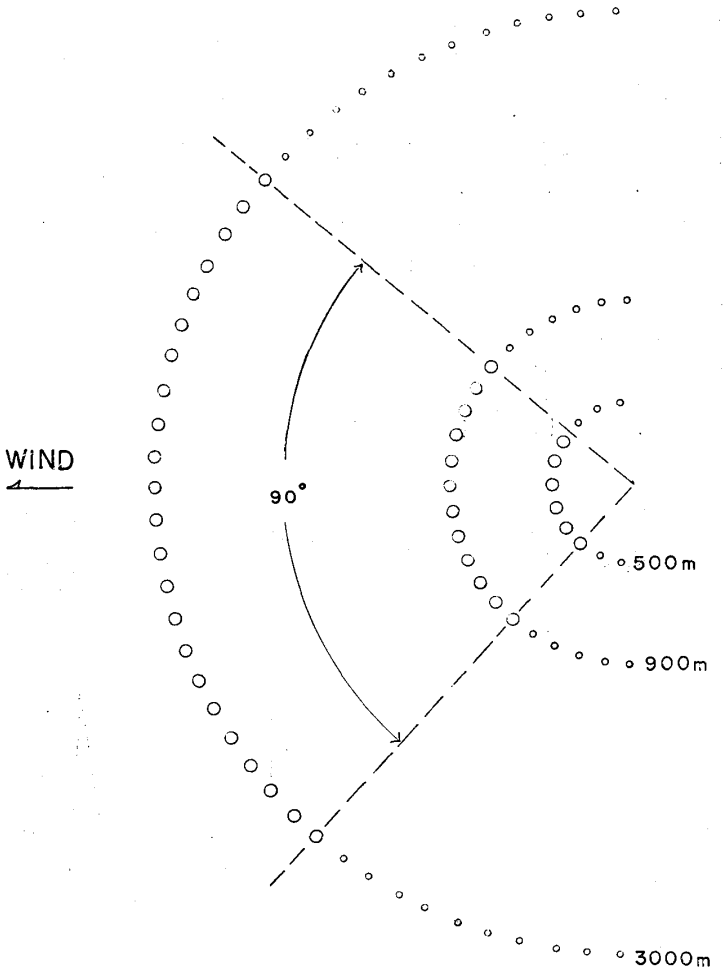

Fig. 1. Arrangement of the measuring posts.

Owing to the complexieties caused by the nature of the phenomena itself, and caused by the difficulties of the concentration measurements of ice crystals, there may be some discordances; however, we can notice clearly the substantial characteristics that the positions of the maxima and minima of the curves for each distance coincide with each other; so these characteristics might not be considered as the results of accident.

Such characteristic features which are dependent only on the azimuthal angles indicate that the cause which results these distributions effects on a scale covering over the whole field of the experiments. Therefore, the cause may chiefly be the change or meandering of the wind direction which occurs simultaneously over the whole field.

In the February experiments, ice crystals of PbI_2 were emitted from the source at the height of 1.5 m above the ground and were sampled at the posts in every 8～10°ca. on 50, 100 and 300 m ca. arcs. The horizontal concentration profiles on the 50 m arc were

Table 1. Table of the fundamental data of the experimental conditions.

No. of Exp.	Date	Source Intensity (unit/sec)	Wind Speed (u) (m/sec)							Air Temp (T) (°C)				$\frac{\partial T}{\partial \log_{10} z}$	$\frac{V_*}{\kappa}\log_{10}\frac{Z_0}{}$	ζ	Insolation (gcal/cm²/h)
			Tower				Pilot balloon			Tower							
			10m	20m	45m	65m	Tokai Middle School	Post No. 217	Mean (Used for calculation)	0.5m	10m	20m	40m				
I	June 1 1200 ~ 1210	1.10×10^{10}	1.8	2.3	2.5	2.9	5.5	6.2	2.38	20.8	19.7	19.8	19.1	−0.70	1.4	−0.35	86.4
II	June 2 1200 ~ 1210	3.35×10^{10}	1.9	1.9	2.1	2.3	2.3	2.0	2.05	17.8	17.1	17.0	16.6	−0.60	1.65	−0.22	19.2
III	June 3 1200 ~ 1210	6.71×10^{10}	4.2	6.4	6.6	6.6	4.4	12.5	6.0	18.6	17.0	16.7	16.4	−1.10	2.5	−0.175	105.4
VI	June 4 1230 ~ 1250	8.62×10^{10}	5.1	7.4	8.5	8.1	6.2	7.8	7.3	17.5	16.5	16.3	15.6	−1.00	2.55	−0.154	96.0

Fig. 2~5. Concentration distribution. χ: number/litre.

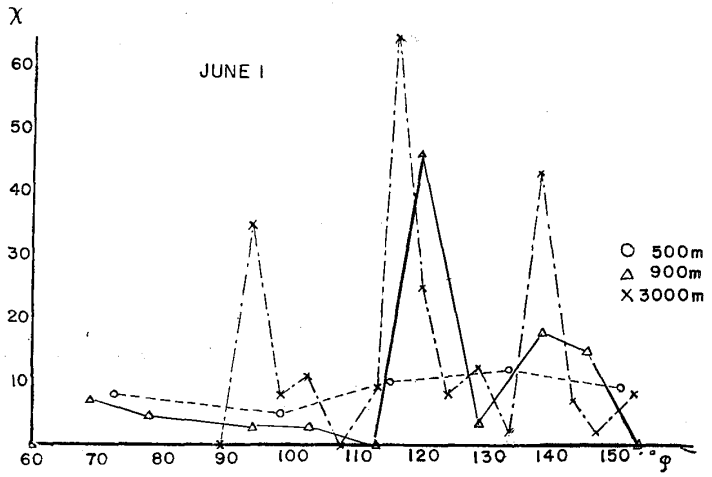

Fig. 2.

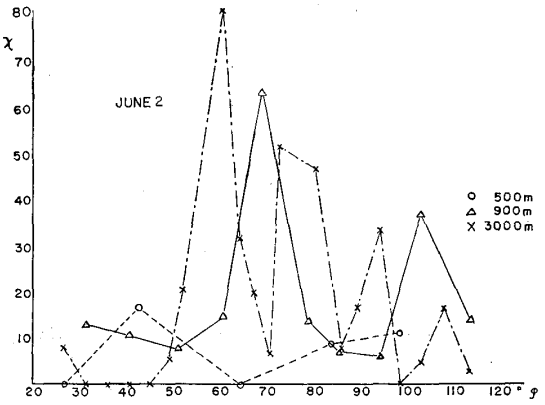

Fig. 3.

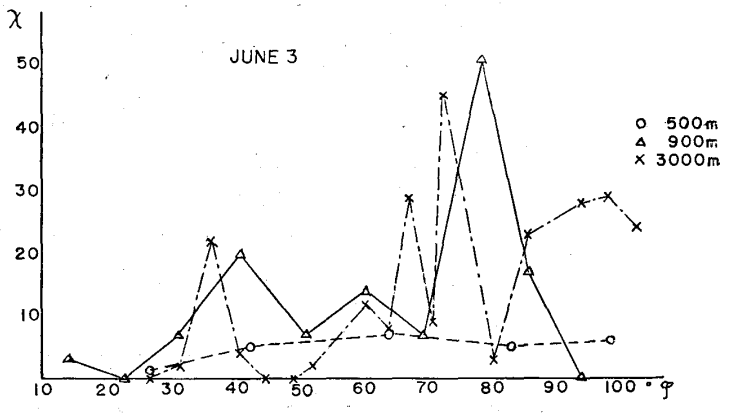

Fig. 4.

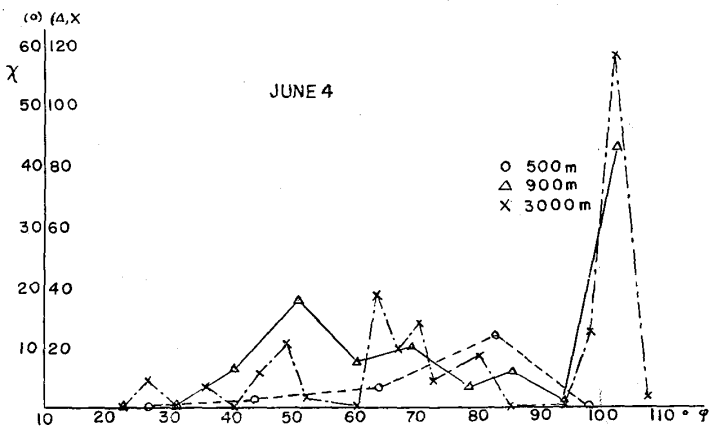

Fig. 5.

Fig. 6~9. Resemblance between the concentration distributions at each leeward distance.

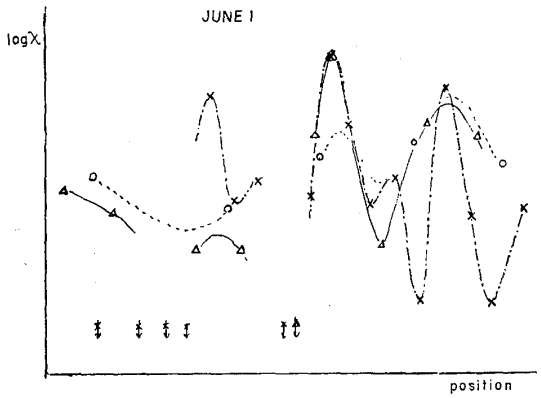

Fig. 6.

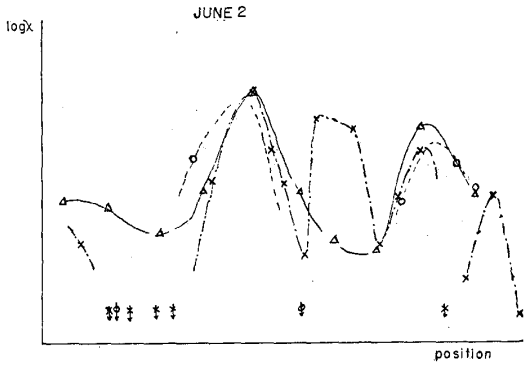

Fig. 7.

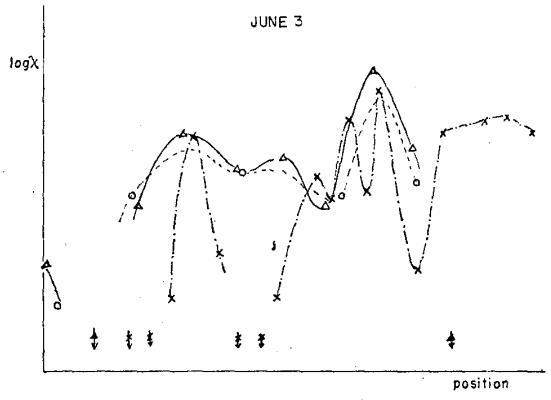

Fig. 8.

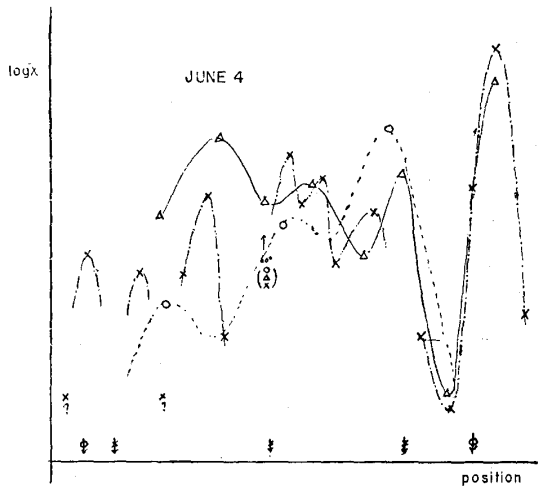

Fig. 9.

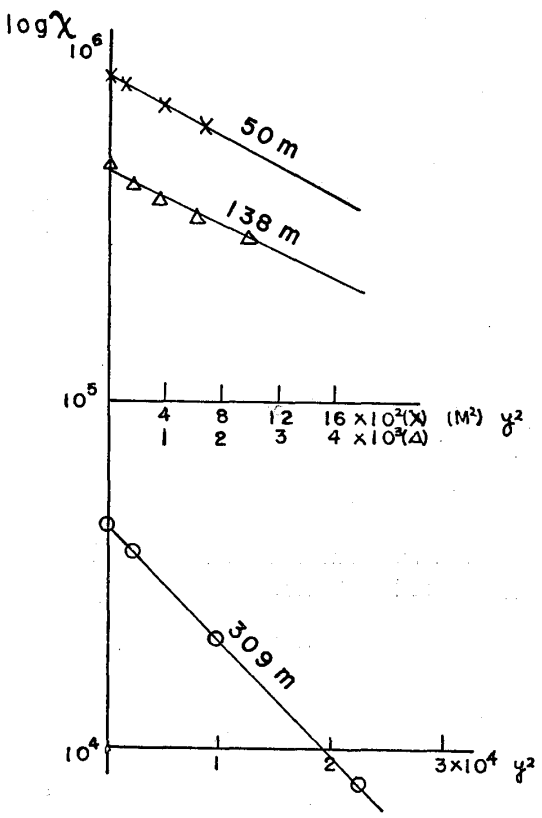

Fig. 10. Relations between log x and y^2 in the February experiment.

regarded as normal (Fig. 10), but in the June experiments, as above mentioned, the profiles had many unevennesses, and differred considerably from the normal distribution.

The frequency distributions of the wind directions obtained from the records in every 1 sec of the quick running charts of the wind vane at the source showed that they were nearly normal (Fig. 11), and they had not any resemblance to Figs. 5~9. Therefore, the above mentioned similarity of the profiles for every distance in the June experiments may not be caused by such a process that the smoke puffs emitted from the source keep the instantaneous initial directions at the source during the whole travel over the field. So another process should be considered.

Let the wind at the source be expressed by a vector $\tilde{s}(t)$. According to the assumption that the cause effects uniformly over the whole field, the radius vector, its origin is at the source, which indicates the position of a puff emitted from the source may be expressed by

$$\tilde{r}(t)=\int_0^t \tilde{s}(t)dt \tag{1}$$

The angular position φ of the puff which reached at the leeward (radial) distance ρ may be expressed by

$$\varphi(t)=\arg[\tilde{r}_\rho(t)]=\arg\left[\int_0^{t_\rho}\tilde{s}(t)dt\right] \tag{2}$$

where t_ρ is calculated by

$$\left|\int_0^{t_\rho}\tilde{s}(t)dt\right|=\rho \tag{3}$$

The emitting period of the source is assumed to be sufficiently large and the sampling of the puff begins at t_1 and ends at $t_2=t_1+T$, then the instantaneous angular position $\varphi(\xi)$ on the arc of distance x is

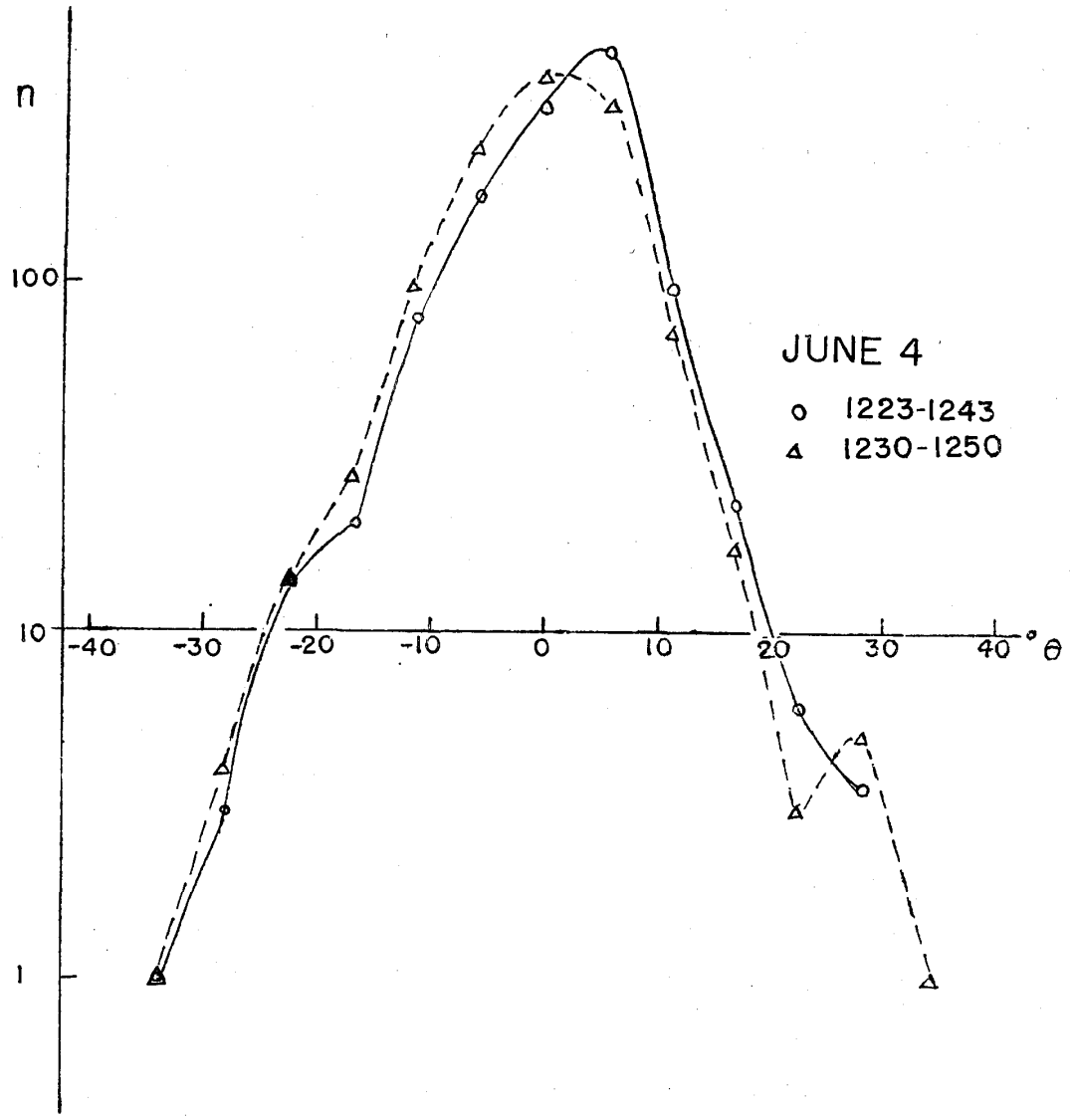

Fig. 11. Frequency distributions of the wind directions.

given by

$$\varphi(\xi) = \arg\left[\int_{t_1-t_x+\xi}^{t_1+\xi} \tilde{s}(t)dt\right] \qquad 0 \leqq \xi \leqq T \tag{4}.$$

It is very diffucult to carry out the calculations using Eqs. (1) to (4), so we assume further as a first approximation that

$$|\tilde{s}(t)| = \text{constant} = \bar{u} \tag{5},$$

where $\bar{u}$ is the mean wind speed. Then we can write

$$\tilde{s}(t) = \bar{u}\tilde{\theta}(t) \tag{6},$$

$\tilde{\theta}(t)$ is an angular vector. Furthermore, we assume that the process goes on almost stationarily, Eq. (3) becomes

$$\bar{u}\left|\int_{t_1+\xi-t_x}^{t_1+\xi}\tilde{\theta}(t)dt\right| \fallingdotseq \bar{u}\left|\int_{t_1-t_x}^{t_1}\tilde{\theta}(t)dt\right| = x \tag{7},$$

and, as the error which occurs by assuming $\sin\theta=\theta$ is less than 10% even when $\theta=45°$, we obtain that

$$t_x = x/\bar{u} \tag{8}$$

and

$$\varphi(\xi) = \arg\left[\bar{u}\int_{t_1-\frac{x}{\bar{u}}+\xi}^{t_1+\xi}\tilde{\theta}(t)dt\right] = \mathrm{Sin}^{-1}\left[(\bar{u}/x)\int_{t_1-\frac{x}{\bar{u}}+\xi}^{t_1+\xi}\sin\theta(t)dt\right]$$

$$= \int_{t_1+\frac{x}{\bar{u}}+\xi}^{t_1+\xi}\theta(t)dt \Big/ (x/\bar{u}) \tag{9}.$$

Occurrence frequencies of φ during t_1 to t_2 express the horizontal concentration profiles and Eq. (9) indicates that φ is able to be calculated by taking a moving average of interval $x/\bar{u}$ from the record of the wind direction at the source.

When $x/\bar{u}$ is small,

$$\varphi(\xi) = \frac{\bar{u}}{x}\int_{t-\frac{x}{\bar{u}}+\xi}^{t+\xi}\theta(t)dt \fallingdotseq \frac{\bar{u}}{x}\frac{d}{dt}\left(\int_{t-\frac{x}{\bar{u}}+\xi}^{t+\xi}\theta(t)dt\right)\frac{x}{\bar{u}} = \theta(t+\xi) \tag{10}.$$

So $\varphi(\xi)$ coincides with $\theta(t+\xi)$ and the concentration profiles near the source show nearly the same frequency distribution of the wind directions which arc usually normal. Generally $\theta(t)$ can be expressed by a Fourier series in t:

$$\theta(t) = \frac{a_0}{2} + \sum(a_n\cos nt + b_n\sin nt) \tag{11}.$$

Considering $\Phi(\xi)$ which corresponds to Eq. (10),

$$\Phi(\xi) = \frac{1}{\tau}\int_{\xi-\tau}^{\xi}\theta(t)dt \tag{12},$$

we obtain

$$\Phi(\tau) = \frac{a_0}{2} + \frac{1}{\tau}\sum\frac{1}{n}[a_n\{\sin n\xi - \sin n(\xi-\tau)\} - b_n\{\cos n\xi - \cos n(\xi-\tau)\}]$$

$$= \frac{a_0}{2} + \frac{1}{\tau}\sum\frac{2}{n}\sin\frac{n}{2}\tau\left[a_n\cos n\left(\xi-\frac{\tau}{2}\right) + b_n\sin n\left(\xi-\frac{\tau}{2}\right)\right] \tag{13}.$$

Therefore, if $\tau = x/\bar{u}$ is given, some components in the series vanish when

$$n = 2m\pi/\tau \quad (m: \text{integer}) \tag{14}.$$

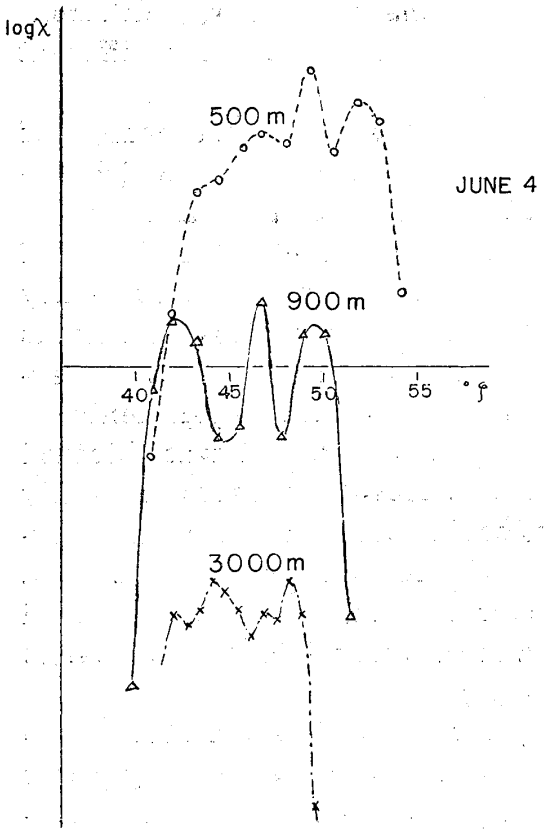

Fig. 12. Frequency distributions ($\propto\chi$) of the angle φ.

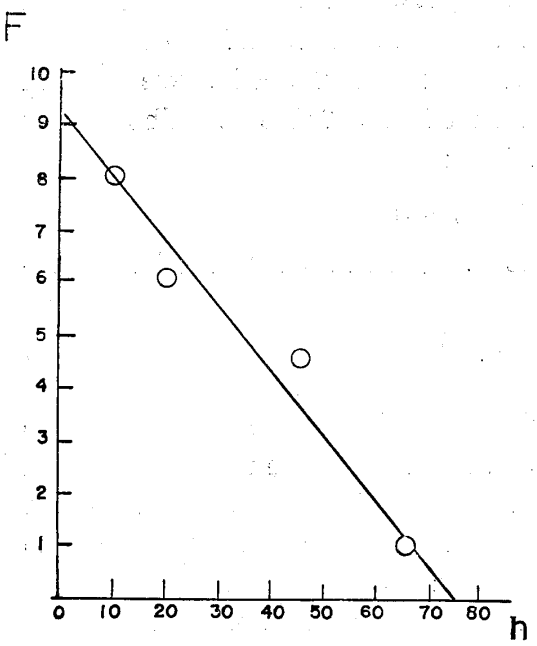

Fig. 17. Relation between F and h.

Fig. 13—16. Record of the wind vane at each height.

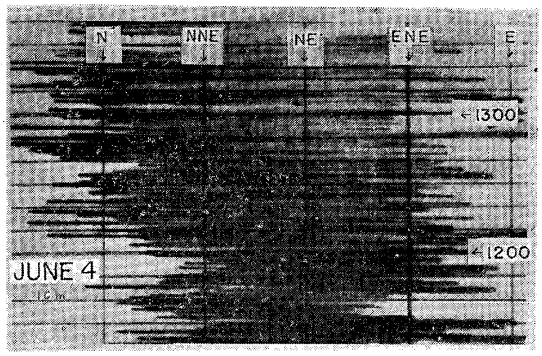

Fig. 13. (10 m)

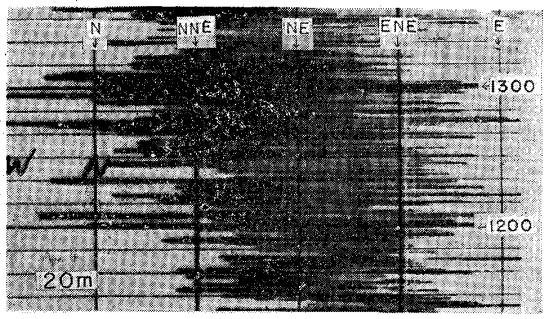

Fig. 14. (20 m)

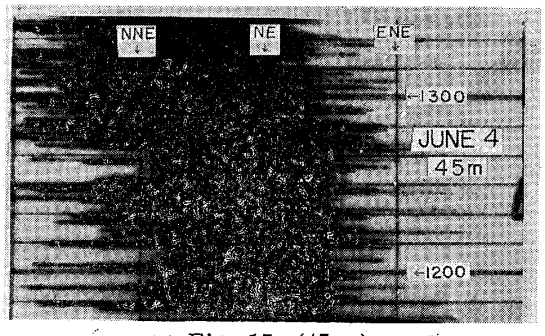

Fig. 15. (45 m)

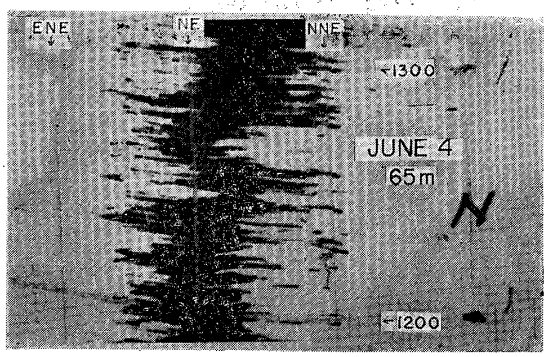

Fig. 16. (65 m)

Table 2. Table of Ψ and F.

z (m)	10	20	45	65
ψ (o)	72	54	41	9
F	8.1	6.1	4.6	1

So it is probable that even from the same function $\tilde{s}(t)$, different profiles may result for different travel distances.

The effect of the change of the wind directions which has influences on the horizontal concentration profiles should be averaged over the height between the height of the source (65 m) and that of the sampling posts. In order to obtain such results, it is necessary to set several wind vanes with quick running devices in various heights, but such an instrumentation might generally not be expectable in many experiments including these June experiments.

Unfortunately, in these experiments, such a record was obtained only at 65 m high above the ground and, moreover, there was only one record on June 4 with which we could carry out such an analysis. So we must evaluate the averaged effects from the data at a single height. We calculated the occurrence frequencies of the wind directions of June 4 in every 5 sec and in every 0.562°, with $\bar{u}=7.3$ m/sec and $T=20$ min. (cf. foot note (2))

The frequency distributions of φ for $x=500$, 900 and 3000 m are shown in Fig. 12. Inspite of the same sampling period, they differ from Fig. 11. The resulted ranges of φ are 8°～14° which are considerably different from 90° ca in Fig. 5～9.

The records of the wind vane in usual speed at 10, 20, 45 and 65 m are shown in Figs. 13～16, and it is obvious that the ranges of the variations clearly decrease with the heights, and the range at 65 m is markedly narrow comparing with other records. If we measure the ranges (ψ) of the bandshaped parts of the records, we obtain the results shown in the 2nd column of the Table 2. The ratios (F) of ψ at each height to that at 65 m.;

$$F=\psi_i/\psi_{65} \quad (i=10,\ 20,\ 45) \tag{15}$$

are shown in the 3rd column in Table 2. F can be regarded approximately as

$$F=9.2-9.2\ \mathrm{h}/75 \tag{16}$$

(Fig. 17).

The magnitude of the vertical diffusion has been considered as it increases with the height. The author obtained the diffusion formulae in 1933 with the diffusion coefficient proportional to the height, and the formulae thus obtained express fairly good the results of experiments.[3),4),5)] Therefore, the time during which the horizontal wind direction is effective to the vertical diffusion is larger in lower heights than in upper heights. So, as for the averaged effects, a weighing factor which is larger in lower heights

should be considered. We adopt the weighing factor ω:

$$\omega = 1/h \tag{17},$$

so the weighted mean of F becomes

$$\bar{F} = \frac{\int_2^{65} F\omega dh}{\int_2^{65} \omega dh} = 9.2 - \frac{9.2}{75}\,\frac{63}{\log(65/2)} = 7.0 \tag{18}.$$

By multiplying this factor $\bar{F}$ to the results shown in Fig. 9, we obtained Fig. 18, and this shows nearly the same features of Fig. 9.

Thus the detailed features of the horizontal concentration pro-

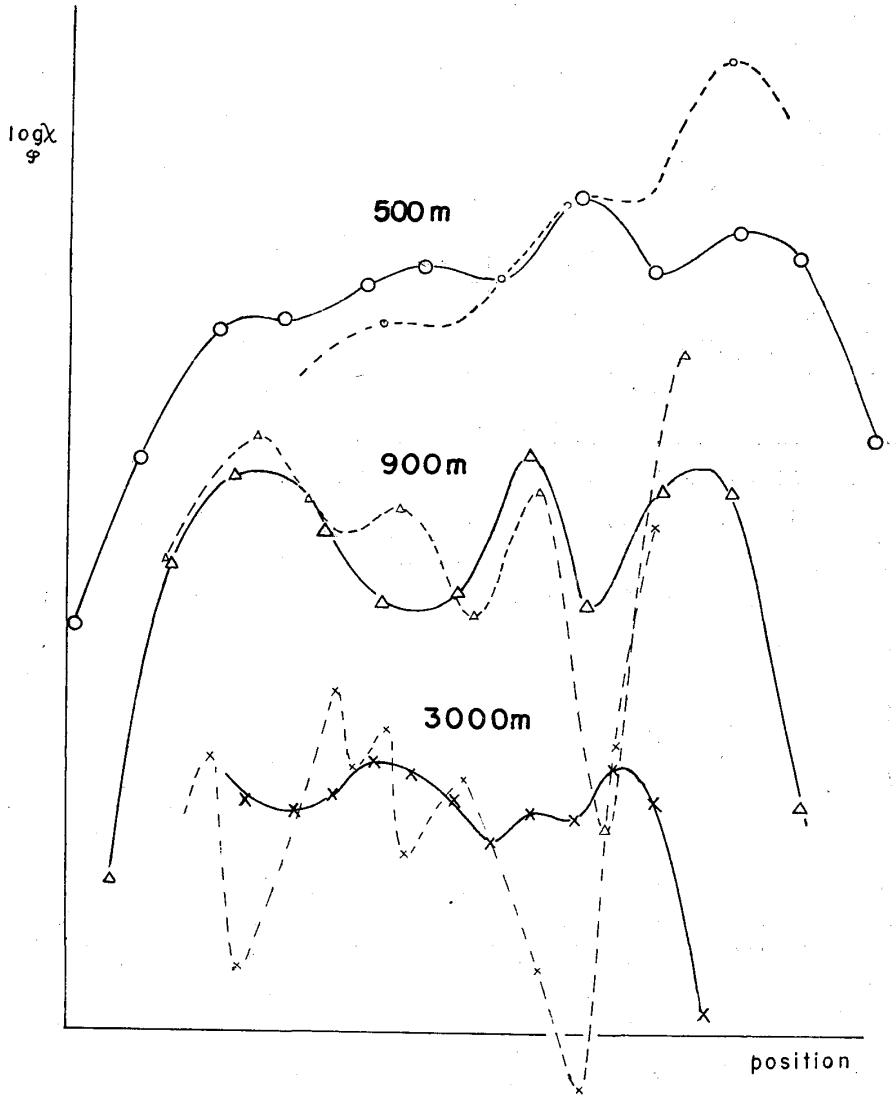

Fig. 18. Corrected distributions of the angle φ (broken line) and the measured concentration distributions (solid line).

files can be estimated from the data of the wind vane, but it may also be necessary to treat the profiles more macroscopically. The profiles show in the main the plateau type except in the near region of the source, so in order to measure the degree of the horizontal diffusion, we should adopt a quantity L, which is the width between both ends where the concentration is 1/10 of the peak concentration. We plotted L against x for each run, we obtain the marks ○ in Fig. 19. If we assume that the Lagrangian correlation is proportional to $\exp(-\xi)$, and transforming t to $x/\bar{u}$, we obtain from the Taylor's equation:

$$\bar{y}^2 \propto (\varphi_A x + e^{-\varphi_A x} - 1) \tag{19}$$

We assume that L^2 has the same charactor as $\bar{y}^2$, and we put

$$L^2 = q_A(\varphi_A x + e^{-\varphi_A x} - 1) \tag{20}$$

From the results given in Fig. 19, we could determine the values of $\sqrt{q_A}$ and φ_A (Table 3).

Table 3. Table of $\sqrt{q_A}$ and φ_A.

Run	I	II	III	IV
$\sqrt{q_A}$ (10^3)	8.3	4.6	5.3	2.1
φ_A (10^{-4})	4.56	3.0	3.53	6.45

The calculated results by using Eq. (20) and the values thus determined are shown as the curves in Fig. 19, which indicate the adequateness of Eq. (20) over all region of the experiments.

If we plot accumulated concentrations aginst their lateral distances on "Probability papers" for every leeward distance, we obtain Fig. 20, and the points for each distance show complicated unevenness and do not arrange themselves on a straight line, so we cannot assume the normal distribution. But if we regard very roughly that these results show the normal distribution, we shall adopt the straight lines in Fig. 20, and the values of the standard deviation $\sqrt{A}$ may be determined. (Table 4).

Table 4. Standard deviations of the lateral spread.

Run \ x (m)	500	900	3000
I	353	427	1095
II	295	427	1321
III	213	376	1422
IV	149	694	1990

The relation between $\sqrt{A}$ and x are shown by the marks △ in Fig. 19. The marks ○ indicate the results of L already mentioned. All the four experiments were carried almost in the same meteorological

conditions, but the inclinations of the lines for $\sqrt{A}$ variate more considerably than those for L. So L seems to be more suitable quantity than $\sqrt{A}$ in order to measure the degree of the horizontal diffusion in a rather far region.

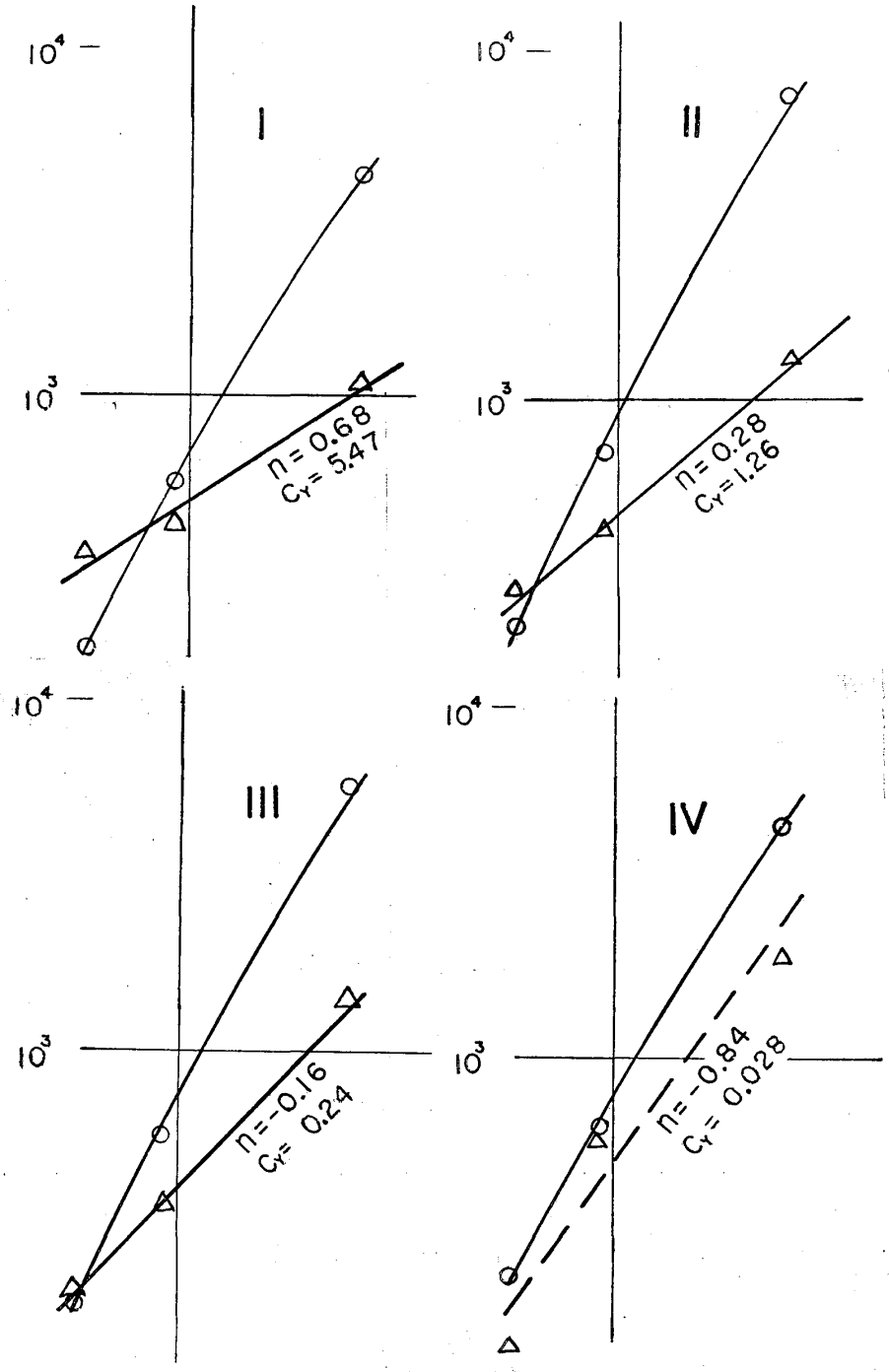

Fig. 19. Curves of L and $\sqrt{A}$ versus x.(○ : L, △ : $\sqrt{A}$).

Fig. 20. Curves of the accumulated concentrations versus the lateral distances.

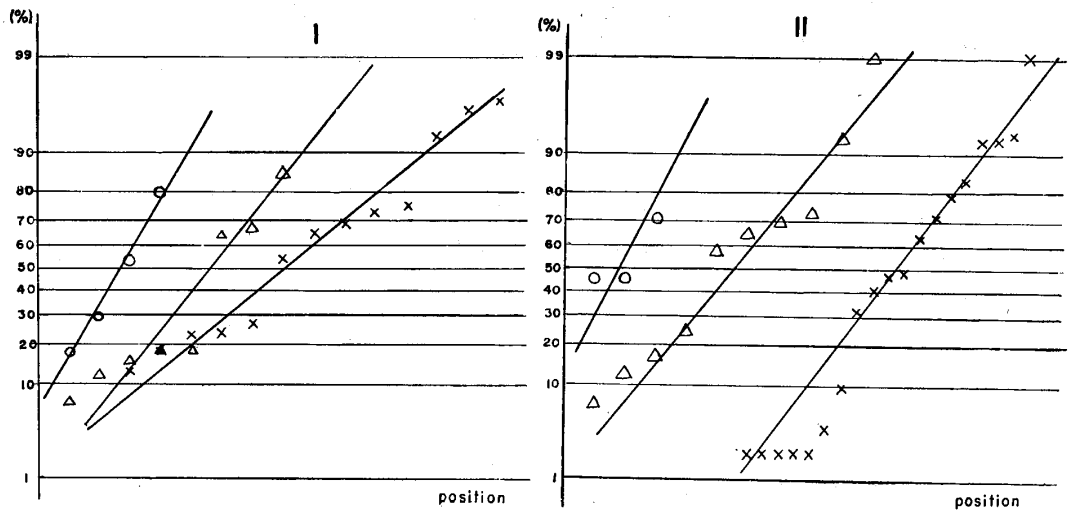

Fig. 20 (a).

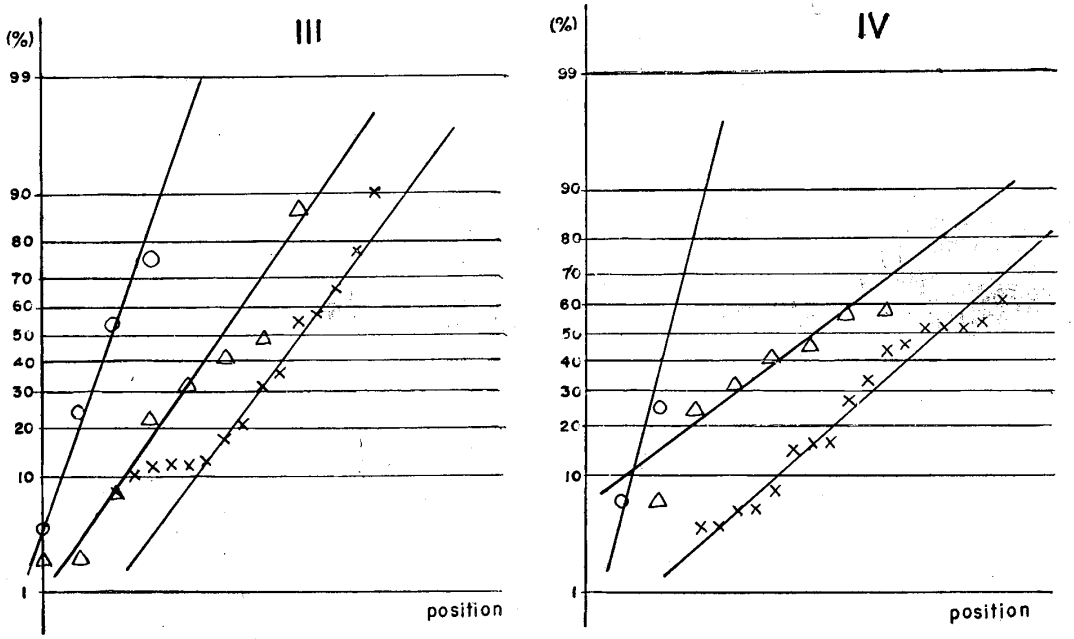

Fig. 20 (b).

Vertical concentration profiles

The same treatment, as mentioned above for the horizontal profiles, should be adopted for the vertical concentration profiles, by using the data of bivane, but it was impossible because we had no result of vertical concentration measurements. As the height of the stack, 65 m, however, is nothing but only $65/3000 \fallingdotseq 0.22$ of the whole range, if we consider the whole region up to 3 km, the diffusion phenomena, except in the neighbourhood of the source, should be considered that they occur in a rather low domain, and

that the influence of the ground should be effective, so the effects of variations of the elevation angles do not maintain so longer than those of the azimuthal angles.

χ_{CIC}

To consider the vertical diffusion without the effects of the horizontal diffusion, we adopt, after Cramer,[6] the quantity χ_{CIC}:

$$\chi_{CIC}=\int_{-\infty}^{\infty}\chi dy \qquad (21).$$

We obtained the values of χ_{CIC} from the data given in Figs. 2~5 by graphical integration (Table 5).

Table 5. χ_{CIC}.

Run \ x (m)	500	900	3000
I (10^7)	0.674	1.37	5.32
II (10^7)	0.495	2.72	10.3
III (10^7)	0.377	1.72	6.31
IV (10^7)	0.246	2.60	6.57

This quantity χ_{CIC} is expressed by the author's formula.

$$\chi_{CIC}=\frac{q}{\bar{u}}\frac{1}{B}\exp\left(-\frac{h+z}{B}\right)J_0\left(i2\sqrt{\frac{hz}{B}}\right) \qquad (22),$$

where q is the source strength. By using this formula and the given values of q and $\bar{u}$, we could determine the values of B at each distance. In this case a quesition arise, what values should be adopted as the effective mean wind speeds. It has been varified that the diffusion coefficients should be proportional to the wind speed, [4),5)] so the values of B in Eq. (22) become independent of the wind speed, and the values of the wind speed only determine the dilution rate of the smoke caused by the volume change of smoke-containing air. So we may consider that it is most adequate, if we adopt the average value of the wind speeds at the stack height (65 m) down to the sampling height (2 m). As we had no datum below 10 m, we took the average of the results of 65, 45, 20 and 10 m.

We plotted the calculated results of B against x and obtained Fig. 21. As before, we assume that

$$B=q_B(\varphi_B x+e^{-\varphi_B x}-1), \qquad (23),$$

because we can show that quantity B has the same meaning as the standard deviation,[3] and we could determine the values of q_B and φ_B (Table 6).

Table 6

Run	I	II	III	IV
q_B	1.1	1.8	0.65	0.71
φ_B	0.019	0.012	0.028	0.027
ζ[4]	−0.35	−0.22	−0.23	−0.15

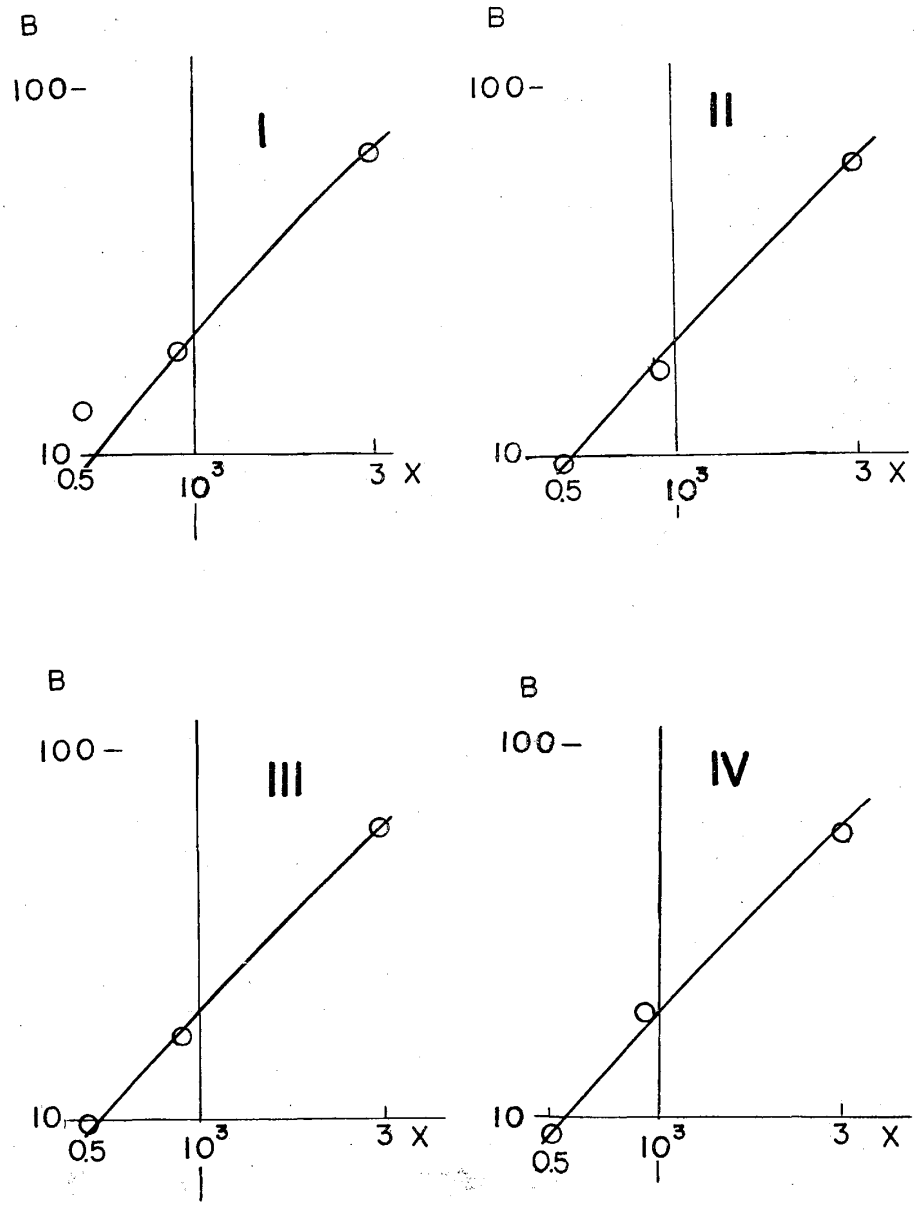

Fig. 21. Curves of B versus x.

(4) ζ is a parameter for the meteorogical conditions defined by $\zeta = \frac{\partial T}{\partial \log_{10} z} \Big/ \left(\frac{V_*}{\kappa} \log_{10} z_0\right)^2$, assuming that both profiles of wind speed and temperature take the forms of logarithmic distribution.

The ζ-dependencies of both quantities q_B and φ_B have been discussed in the former report[3].

The curves in Fig. 21 are calculated from Eq. (23), using the values of q_B and φ_B in Table 6. These functional forms of Eqs. (22) and (23) should be regarded as adequate ones over all regions of the experiments.

In conclusion, the author's formulae express fairly well all the data of the observation over the whole field of the experiments.

Discussions about the Pasquill's method

A method of concentration estimation—Pasquill's method—has been reported by Maede,[7] and in our country it is commonly called as the English method. According to this method, 1) the meteorological conditions are classified into 6 categories: A~F by using the wind speeds and insolations. 2) The plume is assumed to have a profile of the normal distribution; and the angle θ which subtends both ends of the plume at which the concentration is 1/10 of the peak concentration is given by a table. 3) The plume heights (h) are given for the leeward distances from the source and for each category by a diagram. 4) When the source is at the height H from the ground, a table of correction factor ($F(h/H)$) is given as a function of h/H.

Then the method suggests that the peak concentration χ_0 is given by the next formula:

$$\chi_0 = \frac{2.8 \times 10^{-3}}{\bar{u} d \theta h} \tag{24}$$

where d is the leeward distance (km), and the source strength is assumed 1 unit/min.

All the four experiments in June were regarded to be in the category D. If we assume very roughly the normal horizontal profile, the observed results of θ were 60~130° for all distances, but the table shows its values as 15~18°.

According to this method, the concentrations may be expressed by

$$\chi = \frac{q}{\bar{u}} \frac{2.8 \times 10^{-3}}{d \theta h} F\left(\frac{h}{H}\right) e^{-\frac{y^2}{A}} \tag{25}$$

If we measure d in meter, θ in radian, and put them d' and θ respectively, we obtain

$$\chi = 2.97 \times \frac{q}{\bar{u}} \frac{F\left(\frac{h}{H}\right)}{d'\theta' h'} e^{-\frac{y^2}{A}} \tag{26},$$

and we get

$$\chi_{CIC} = \int_{-\infty}^{\infty} \chi dy = 2.97 \times \frac{q}{\bar{u}} \frac{1}{d'\theta' H} \frac{F(\eta)}{\eta} \sqrt{A\pi} \tag{27},$$

where $\eta = h/H$. From the assumption of the normal distribution, we have the relation that $\exp(-(d\theta'/2)^2/A) = 0.1$, so

$$d'\theta' = 2\sqrt{A} \times \sqrt{2.303} \tag{28},$$

then we can get

$$\chi_{CIC} = 1.732 \times \frac{q}{\bar{u}} \frac{1}{H} \frac{F(\eta)}{\eta} = 2.67 \times 10^{-2} \frac{q}{\bar{u}} \frac{F(\eta)}{\eta} \tag{29},$$

because H is 65 m in this case. Finally we get

$$\frac{\chi_{CIC}}{q/\bar{u}} = 2.67 \times 10^{-2} \frac{F(\eta)}{\eta} \tag{30}.$$

We calculated these quantities for each distance and for category D, togather with for categories C and E (Fig. 22).

The Committee has made the conclusion that this method was applicable within the allowance limits of $10^{\pm 1}$. That conclusion may be valid, but this method does not seem to be so powerful to be adopted to the phenomena on the further large scale.

Sutton's formula

As for the horizontal profiles, Sutton's formula[8] shows that

$$\chi \propto \exp\left(-\frac{y^2}{A}\right), \qquad A = C_y^2 x^{2-n} \tag{31}.$$

From Fig. 19, we can determine the values of n and C_y. The values of n variate from 0.6 to even the negative value -0.7, while the usually assumed values for lapse conditions are 0.2~0.35.

As for the vertical profiles, the Sutton's formula for χ_{CIC} is given by

$$\chi_{CIC} = \frac{q}{\bar{u}} \frac{1}{\sqrt{\pi B}} \left(\exp\left(\frac{(h+z)^2}{B}\right) + \exp\left(-\frac{(h-z)^2}{B}\right) \right)$$

$$B = C_z^2 x^{2-n} \tag{32}.$$

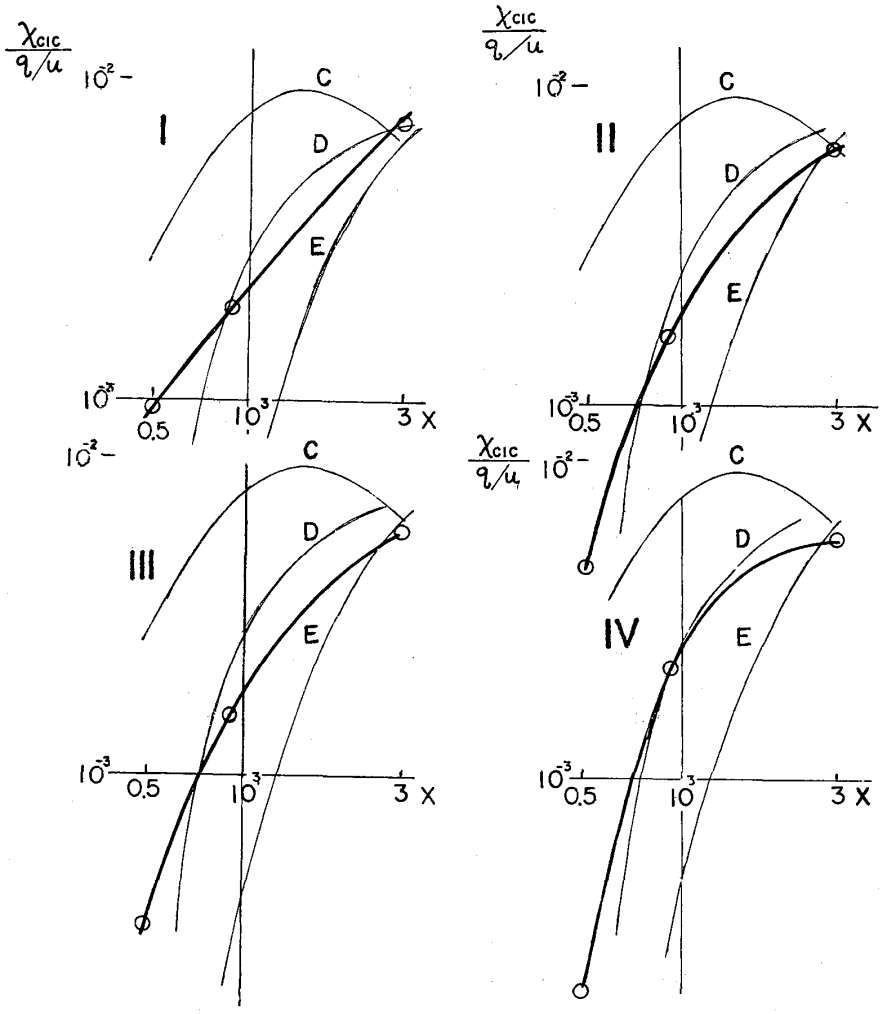

Fig. 22 Curves of $\chi_{CIC}/(q/u)$ versus x.

From the observed data, we could calculate the values of B for every distance in each experiment. The results are shown in Fig. 23 and we can see that the values of n variate from 0.95 to 1.20, which are very different from the usually assumed values 0.2～0.35, and that even for each experiment, the values of n for horizontal and vertical diffusion differ considerably each other.

So the Sutton's formula and the usually assumed values of the parameters do not seem to fit well.

Conclusion

Because of the difficulties caused chiefly by economical reason, the vertical concentration profiles were not observed and all the four experiments were carried almost in the same meterological conditions, so there might have been some insufficiencies from the pure scientific point of view. However, the experiments carried out

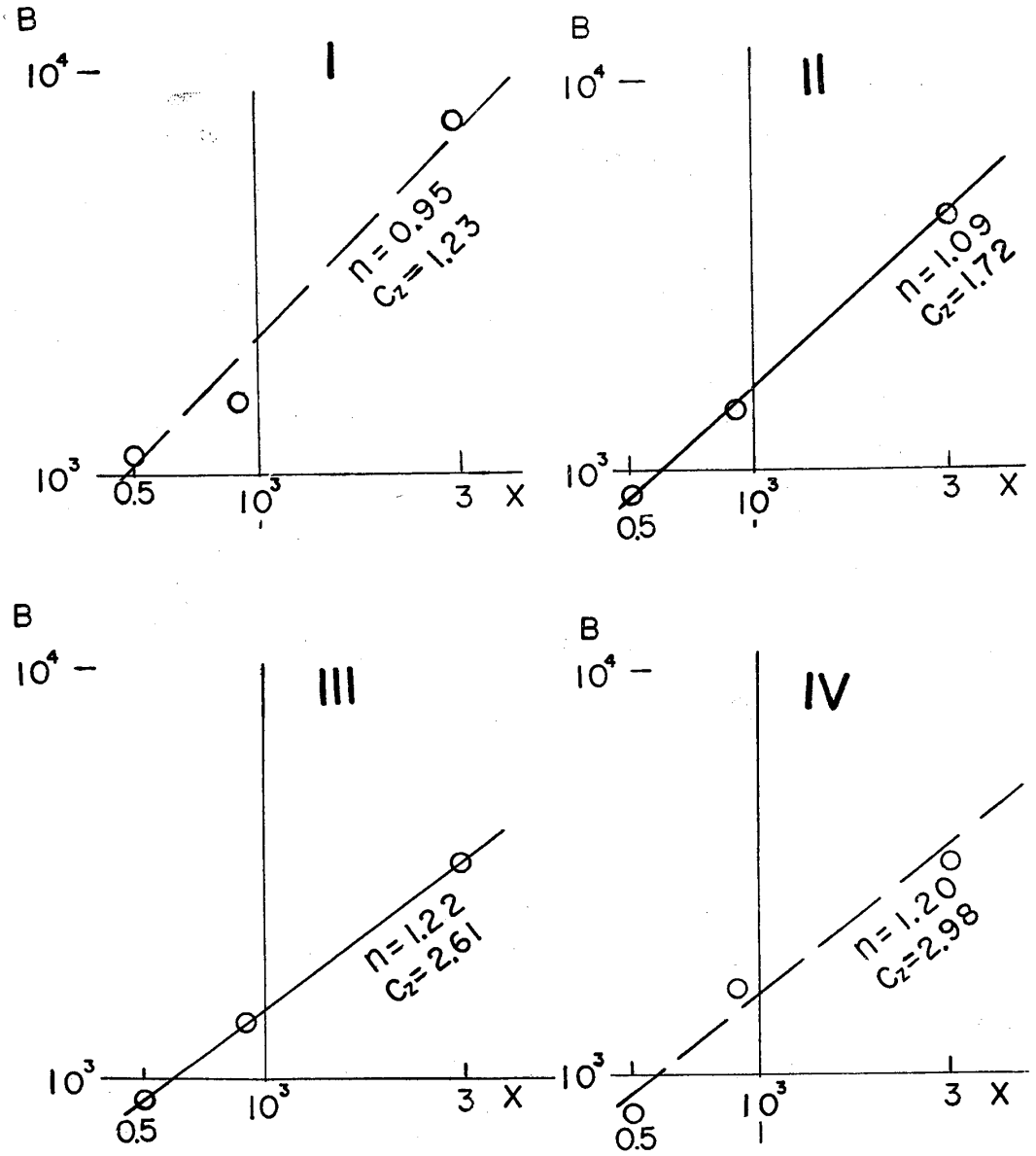

Fig. 23. Curvse of B versus x (Sutton's formula.)

in Tokai have presented valuable data for the atmospheric diffusion within the range of 3 km.

As the conclusion of these analyses, the author's formulae showed fair agreements with the results of the experiments, just as in the case of the analyses of the Prairie Grass Project.

References

1) 原子力気象調査会： 東海村原子力気象調査 ― 東海村の煙突から出る廃棄物の拡散に関する調査, 昭和 34 年 12 月

2) Kawabata, S.: Observations of Atmospheric Diffusion at Tokai-mura, Geophy. Mag., 29 (4) 1960, 571-582

3) Sakagami, J.: On the Relations between the Diffusion Parameters and Meteorological Conditions, Natural Sci. Rep. Ochanomizu Univ., 11 1960, 127-158
4) Sakagami, J.: On the Turbulent Diffusion in the Atmosphere Near the Ground, ibid., 5 1954, 79-91
5) Sakagami, J.: On the Atmospheric Diffusion of Gas and Aerosol Near the Ground, ibid., 7, 1956, 25-61
6) Cramer, H. E., Record, F. A. and Vaughan, H. C.: The Study of the Diffusion of Gases or Aerosols in the Lowest Atmosphere, Final Rep., No. AF 19 (604)- 1058, G. R. D., 1958
7) Meade, P. J.: The Effects of Meteorological Factors on the Dispersion of Airborne Material, Paper presented to the International Symposium on Safety and Siting of Nuclear Plants, Rome, June 1959
8) Sutton, O. G.: A Theory of Eddy Diffusion in the Atmosphere, Proc. Roy. Soc., A 104 1923, 640-654

(*Received March 20, 1961*)